Journal of
Smoking Cessation

ARTICLE

Open Access

https://doi.org/10.48130/jsc-0025-0004
Journal of Smoking Cessation **2025**, 20: e004

Insular radiomic features associated with abnormal functional connectivity in individuals with nicotine addictions

Huiling Zheng[1], Qianbiao Gu[1], Haobo Chen[1], Ruotong Zhu[1], Feng Huang[1,2], Peng Liu[1,2], Yanhui Liao[1,2,3*] and An Xie[1,2*]

[1] *Department of Radiology, The First Affiliated Hospital of Hunan Normal University (Hunan Provincial People's Hospital), Changsha 410005, Hunan, China*
[2] *Center for Mind & Brain Sciences, Hunan Normal University, Changsha 410005, Hunan, China*
[3] *Department of Psychiatry, Sir Run Shaw Hospital, School of Medicine, Zhejiang University, Hangzhou 310000, Zhejiang, China*
* Corresponding authors, E-mail: liaoyanhui@zju.edu.cn; xiean@hunnu.edu.cn

Abstract

The insula is a key brain region for internal connectivity and is involved in addiction-related reward systems. Previous studies have revealed abnormalities in insula structure and function in individuals with nicotine addiction (NA); however, few studies have focused on changes in radiomic features of the insula in individuals with nicotine addictions. Therefore, we mined radiomic features of the insula and their relationships with abnormal insula functional connectivity and different smoking characteristics. We recruited 97 volunteers (50 smokers and 47 nonsmokers) and acquired the 3D T1-weighted images (3D T1WI) and the resting-state functional magnetic resonance images (rs-fMRI). On 3D T1WI, insula-based radiomic features were selected via the least absolute shrinkage and selection operator (LASSO), and a support vector machine (SVM) classification model was constructed to distinguish between smokers and nonsmokers. On rs-fMRI, differences in functional connectivity between smokers and nonsmokers were compared by a functional connectivity analysis method based on the insula as a seed point. We correlated radiomic features of the insula between smokers and nonsmokers with functional connectivity differences and smoking characteristics. The SVM classification model that was constructed based on the radiomic features of the insula was able to accurately discriminate between these two populations (area under the curve ROCs of 0.9455 for the training set and 0.8756 for the validation set), and the functional connectivity of the insula to the whole brain differed between smokers and nonsmokers. Radiomic features of insula heterogeneity were associated with a correlation with the smoking index ($r = 0.404$, $p = 0.013$), years of smoking ($r = 0.362$, $p = 0.015$), subjective craving ($r = 0.320$, $p = 0.036$), age at first smoking/first cigarette ($r = 0.302$, $p = 0.036$), and enhanced functional connectivity of the insula with the right occipital lingual gyrus ($r = 0.288$, $p = 0.044$). We used a machine learning-based data classification method for radiomic features to reveal alterations in insular radiomic features in individuals with nicotine addictions, which may provide a valuable method for exploring the microstructures of individuals with nicotine addictions and providing imaging markers for smoking cessation and tobacco control in addition to clinical indicators. This trial is registered with clinicaltrials.gov (NCT05788068).

Citation: Zheng H, Gu Q, Chen H, Zhu R, Huang F, et al. 2025. Insular radiomic features associated with abnormal functional connectivity in individuals with nicotine addictions. *Journal of Smoking Cessation* 20: e004 https://doi.org/10.48130/jsc-0025-0004

Background

Nicotine addiction (NA) is a mental disorder of physical and mental dependence caused by the long-term use of tobacco, which is mainly manifested by a strong craving for tobacco and uncontrollable behaviors, which cause serious negative impacts on human health and quality of life[1]. Despite the desire of most smokers to quit, relapse rates remain high. Nicotine promotes relapse by activating the 'reward circuit'[2] between the limbic system and the frontal cortex, thus enhancing the individual's experience of pleasure, which is stored in the memory. As an important component of the limbic system, the insula plays a key role in addictive behavior, especially in the perception and regulation of intrinsic states, contexts involving rewards, impulse control, and emotional responses[3,4]. In recent years, international journals have continued to provide evidence that damage to the insula undermines addiction to smoking. Compared to damage to other brain regions, damage to the insula makes it easier for individuals with nicotine addiction to succeed in the quitting process[5]. These individuals are less likely to relapse and may even lack the motivation to smoke again. In addition, deeper transcranial magnetic stimulation (TMS) of the dorsolateral prefrontal region[6] may produce more effective and long-lasting results in the treatment of nicotine addiction, and the insula[7], which is located in the deeper region, is also under consideration for the treatment of addiction with TMS.

In recent years, many studies have investigated the structure and function of the insula in individuals addicted to nicotine. In studies on the mechanisms of nicotine addiction, direct measurements of the structures of brain regions using voxel-based morphometry (VBM) are generally used to characterize the disease in terms of volume reduction. A study by Chen et al.[8] revealed that smokers had reduced gray matter volume (GMV) in the insula and cingulate gyrus compared to nonsmokers. In another study[9], young smokers had an increased volume of gray matter (GM) in the left lateral shell nucleus and a decreased volume of GM in the left anterior cingulate cortex (ACC) compared to nonsmokers, with insula changes not being detected. VBM does not directly measure complex cortical topology when detecting the volume of brain regions, and microstructural changes caused by neuronal changes and functional activities may not be detectable via this method[10,11]. The automated normalization algorithms of VBM analysis methods may alter the extraction of abnormal cortical topology and reduce the discrimination of fine structures. As a result, most research methods focusing on brain structures have begun to apply surface-based morphometry (SBM). SBM is able to elevate many deep topographies to the surface, thereby identifying more deep features. However, many studies have used only a single metric mean as a brain disease feature; for example, reduced cortical thickness in the insula cortex of smokers is associated with greater nicotine dependence and higher cigarette craving scores[12,13], which does not respond well to the characteristics of the brain regions. Multimodal

neuroimaging techniques have been widely used in neurological disorders; however, conventional images are not able to identify some microscopic changes that occur before the brain tissue undergoes significant deformation, such as the absence of dopaminergic neurons, which represents the main neuropathological hallmark of nicotine addiction. This cumulative effect on the brain tissue leads to changes in the pixel intensities of the images; however, such microscopic changes cannot be recognized by the human eye[14]. However, these changes can form specific texture patterns in the image, which can be captured by texture features[15]. Radiomics[16,17] is an emerging field that combines medical imaging with informatics, statistics, and machine learning to quantify and objectively characterize image heterogeneity by quantifying microscopic changes in medical images that are difficult to assess by the human eye, providing a new approach to precision medicine[18]. Radiomics has been widely used in the field of brain diseases, such as epilepsy[19], multiple sclerosis[20], Alzheimer's[21], and Huntington's disease[22]; however, the heterogeneity of radiomic features for addictive diseases is still unclear[17,23].

Although the importance of the insula has been emphasized in previous studies, most studies of resting-state functional changes in nicotine-addicted populations have focused on brain networks. Li et al.[24] suggested in a significance network analysis that young adult smokers had increased anisotropy scores of reduced functional connectivity and structural fiber bundles between the anterior cingulate cortex (ACC) and right insula in young adult smokers relative to nonsmokers. Little attention has been paid to functional changes in the insula alone. Previous studies have provided valuable evidence for alterations in insula structure[8] and function[24] in nicotine addicts, and the findings have not been well reproducible due to the low sensitivity of VBM measurements compared to SBM[25] as well as the singularity of the metrics for cortical analysis. However, radiomics can observe subtle changes that cannot be observed by the human eye, providing high-dimensional quantifiable imaging metrics to comprehensively assess structural changes, compensating for the inability of VBM to directly measure complex cortical topology and the singularity of SBM metrics. Radiomic features[26] in structural images are extracted by computer algorithms, including the gray-level co-occurrence matrix (GLCM), gray-level dependence matrix (GLDM), gray-level run-length matrix (GLRLM), and neighborhood gray-tone difference matrix (NGTDM). Briefly, the GLCM contains spatial information about the relationship between pairs of pixels with similar intensities, the GLDM describes the relationship between a pixel's intensity and the intensities of its neighboring pixels, the GLRLM measures regions of homogeneous pixels, and the NGTDM evaluates the differences between pixel intensities. Therefore, in this study, we used radiomics to explore the heterogeneity of the radiomic features of the insula. We further used resting-state functional connectivity analysis(rs-fc) based on the insula to assess the relevant functional changes in the insula.

Currently, few studies have focused on the heterogeneity of insula radiomic features and their associated functional connectivity changes in individuals with nicotine addictions. Moreover, few studies have explained these structural and functional changes in relation to smoking characteristics. As a key node in the neural circuit of smoking addiction, the structural and functional abnormalities of the insula play an important role in smoking behavior. In recent years, with the rapid development of imaging technology, neuroimaging has become an important tool for studying the neural mechanisms of smoking behavior. Radiomics is able to extract a large number of quantitative features from structural images, revealing subtle structural changes that cannot be observed by traditional methods, while rs-fc analysis reflects the functional integration and segregation of neural activities by characterizing the dynamic interaction patterns between brain regions. The combination of radiomics and rs-fc can comprehensively reveal the neural mechanisms of smoking behavior from a multimodal perspective, make up for the limitations of a single approach, enrich the characteristic neuroimaging alterations of the insula in nicotine addiction, and provide a scientific basis for the development of more accurate clinical prediction models and intervention strategies.

Materials and methods

Participants

We recruited a total of 97 subjects (50 smokers and 47 nonsmokers; Table 1) via online publicity and billboards. The inclusion criteria for study participants were as follows: 1) Han Chinese; 2) aged 18–45 years; 3) no smoking cessation in the 3 months prior to the start of the study; 4) no substance dependence other than nicotine; 5) junior high school or higher education level; 6) right-handedness; and 7) no contraindications to MRI scanning. Smokers and nonsmokers were excluded if they: 1) had taken psychoactive drugs, such as antipsychotics and antidepressants, within 3 months before enrollment; 2) were receiving medication; 3) had previous or current psychiatric disorders, as well as mental disorders that met the diagnostic criteria of the DSM-5 within two lines and three generations; 4) had organic brain diseases, a history of craniocerebral injuries, or a history of coma; 5) had severe physical illnesses, a history of endocrine disease, or abnormalities in the blood, cardiac, hepatic, or renal function; or 6) were pregnant or lactating. The criteria for the smoking group were as follows: 1) met the DSM-5 diagnostic criteria for traditional tobacco use disorder; and 2) used traditional combustible cigarettes for more than 1 year and smoked no less than 10 cigarettes per day. The criteria for the healthy controls were as follows: 1) never used tobacco products; and 2) did not have any other history of addiction. All of the subjects were confirmed to be free of intracerebral lesions or structural abnormalities before structural image scanning, demographic and clinical behavioral information, as well as MRI data, were obtained; moreover, all of the smokers were assessed for nicotine dependence using the Fagerstrom test for nicotine dependence[27] (FTND). Smoking data (including the smoking index[28], which is calculated as years of smoking × number of smokers per day/20) and other relevant data were recorded for the subjects using a scale method. Subjects were excluded from the study if they demonstrated a head translation of more than 2 mm or a rotational movement of more than 2 degrees during the MRI scan.

MRI data acquisition and preprocessing

Magnetic resonance data acquisition was performed after all of the scale assessments were completed. All of the images were acquired using a 3.0 T Siemens Magentom Trio scanner (Allegra; Siemens, Erlangen, Germany) with an 8-channel head coil at the Hunan Provincial People's Hospital (the First Affiliated Hospital of Hunan Normal University, Hunan, China). A gradient echo (GRE) sequence was used to acquire the 3D T1-weighted images (3D T1WI) structural images with the following parameters: repetition time = 2000 ms, echo time = 2.26 ms, field of view = 256 mm × 256 mm, flip angle = 8°, number of slices = 176, slice gap = 0, voxel = 1 mm × 1 mm × 1 mm, and matrix size = 256 × 256. An echo-planar imaging (EPI) sequence was used to acquire the resting-state functional magnetic resonance images (rs-fMRI) images with the following parameters: repetition time = 2,000 ms, echo time = 30 ms, field of view = 220 mm × 220 mm, flip angle = 90°, number of slices = 36,

time point = 210, voxel = 3 mm × 3 mm × 3 mm, and matrix size = 64 × 64. The subjects were asked to be relaxed, close their eyes, not think about anything, and not fall asleep during the MRI scan. Earplugs and foam pads were used to minimize noise, and head movements.

3D T1WI structural images were preprocessed on Shukun (www.shukun.net), which mainly includes normalization: comparability of images at different time points, and reduction of noise and artifacts in the images. Rs-fMRI images were preprocessed on DPABI (www.rfmri.org) and SPM (www.fil.ion.ucl.ac.uk/spm). The main preprocessing steps included the following: 1) data format conversion of DICOM to NIFIT; 2) removal of the previous ten volumes; 3) time-slice correction; 4) head-motion correction; 5) spatial normalization, which involved matching of the structural and functional image alignments to the Montreal Neurological Institute standard stereotactic space, with a voxel size of 3 mm × 3 mm × 3 mm; 6) smoothing of the kernel parameter to 4 × 4 × 4; 7) low-frequency filtering; and 8) removal of covariates and the extraction of the mean signals of the head movements as covariates via simple linear regression to exclude the influence of these factors on the results.

Radiomic seed-based analysis

This part was carried out in the software platform provided by Shukun. Two-dimensional visualization of 3D T1 images. Area of interest outlining: the insula was outlined and saved by specially trained operators on the imaging data of different subjects. Feature extraction and selection: we extracted image features (https://pyradiomics.readthedocs.io/en/latest/features.html) from different subjects, removed redundant features with Pearson correlation coefficients ≥ 0.9 by Pearson correlation analysis method, and applied the lasso regression analysis method to select five valuable radiomic features. Building machine learning-based classification models: Support vector machines (SVM)[29] are widely used in machine learning. The dataset of 97 subjects was randomly assigned into a training set and a validation set in the ratio of 7:3[30], and a support vector machine classification model was built based on the five radiomicfeaturesselectedabove,inwhichthetrainingsetwassubjected to 5-fold cross-validation to assess the stability and generalization ability of the model and to avoid assessment bias caused by improper segmentation. The classification model was evaluated using the following metrics: accuracy (ACC), sensitivity (SEN), specificity (SPE), and area under the curve ROC (AUC). Gender and age were subjected to multiple linear regression. Finally, we performed a Spearman correlation analysis between the values of the five selected radiomic features and smoking characteristics.

Functional connectivity seed-based analysis

The bilateral insula was selected as the region of interest based on the automated definition of the AAL template. Whole-brain resting-state functional connectivity analysis with the insula as the region of interest was performed based on DPABI[31] in MATLAB 2020b and SPM12, and time series of the whole insula were extracted and Pearson correlation coefficients were calculated with the time series of other voxels. A two-sample t-test matrix (test level $p < 0.05$) was subsequently designed in SPM12 to compare the differences between smokers and nonsmokers. To improve the reliability of the functional connectivity statistics results, we used a two-stage multiple comparison correction strategy based on Random Field Theory (RFT) in the SPM 12 software package. In SPM 12, a cluster formation threshold of $p < 0.001$ (uncorrected) was first set at the voxel level for generating continuously activated clusters; subsequently, family-wise error rate (FWE) correction was implemented at the cluster level, with the significance threshold set at $p < 0.05$. Finally, Spearman's correlation analysis was carried out between the imaging data of the discrepant brain regions and the smoking behavior data.

Statistical analyses

The statistical software SPSS 26 was used to analyze the basic clinical data of the subjects. Demographic information that was significantly different was included in the multiple linear regression. Correlation analysis between radiomic features and clinical features was performed via SPSS 26. We performed Spearman's correlation analysis was performed regarding the five selected radiomic features associated with functional connectivity differences, and Spearman's correlation analysis was also performed with age at first smoking/first cigarette, smoking index, number of years of smoking, subjective craving, and FTND, $p < 0.05$ was considered to indicate a statistically significant difference. False discovery rate was performed on the results of the correlation analysis.

Results

Demographic information

The demographic information and behavioral characteristics of the smoking and healthy control groups are presented in Table 1. A total of 97 subjects (50 smokers and 47 nonsmokers) were included in this study. Statistically significant differences in sex ($p < 0.05$) and years of education ($p < 0.05$) were observed between the smoking and nonsmoking groups, and multivariate linear regression was utilized to exclude the effects of sex and years of education on imaging outcomes.

Radiomic analysis

A lambda plot of the effective radiomic features of the insula is presented in Fig. 1. Additionally, the features selected via LASSO regression analysis are presented in Fig. 2. The identified radiomic features included T1WI_logarithm_firstorder_InterquartileRange (IQR), T1WI_wavelet-HHH_ glszm_SizeZoneNonUniformity (SZNU), T1WI_wavelet-HLH_firstorder_Mean (Mean), T1WI_wavelet-HLH_ glrlm_ShortRunLowGrayLevelEmphasis (SRLGLE), and T1WI_ wavelet-HLH_glszm_SmallAreaLowGrayLevelEmphasis (SALGLE). Figure 3 demonstrates the performance of the support vector machine model based on radiomic features of the insula. The AUC, SEN, SPE, and ACC values of the classification model were 0.9455, 0.9062, 0.9143, and 0.9104, respectively, for the training set, as well as 0.8756, 0.7333, 0.7333, and 0.7333, respectively, for the validation set. There was no causal relationship between sex, age, and radiomic features. The stable classification performance indicates that the defined radiomic features of the insula are capable of distinguishing between smokers and nonsmokers.

Table 1. Demographic and clinical characteristics of the smoking and healthy control groups.

	Smokers	Nonsmokers	*p* value
Number of individuals	50	47	–
Age (year)	29.66 ± 6.63	27.43 ± 4.35	0.201
Gender, male (%)	49 (98.0%)	32 (68.1%)	<0.001
Years of education	15.18 ± 2.96	17.57 ± 1.81	<0.001
Age at first smoking/first cigarette	12.46 ± 7.35	–	–
Smoking in years	14.98 ± 5.27	–	–
Smoking, cigarettes per day	5.1 ± 2.78	–	–
Craving score	17.04 ± 3.56	–	–
FTND	3.84 ± 2.02	–	–

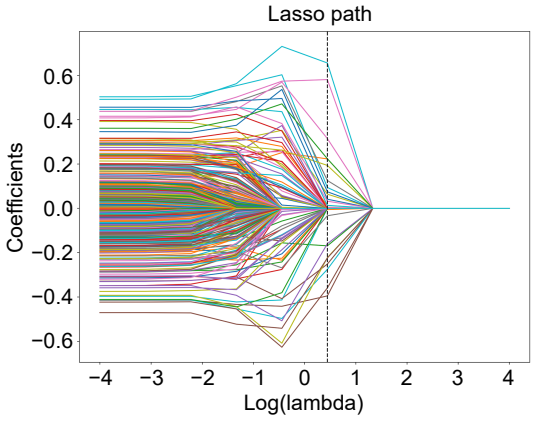

Fig. 1 The coefficient-lambda graph.

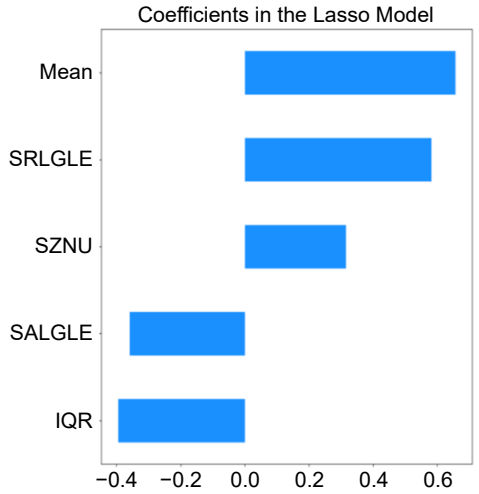

Fig. 2 The selected radiomic features and their specific gravity included in the SVM.

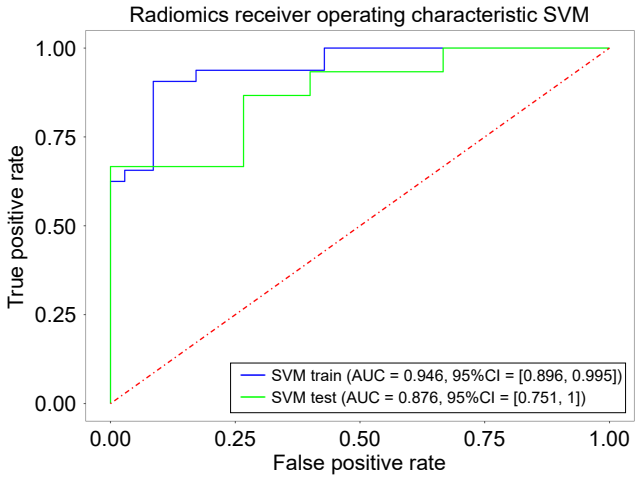

Fig. 3 The ROC curve for categorized smokers vs nonsmokers.

Intergroup differences in functional connectivity between smokers and nonsmokers

Compared with the healthy group, the smoking group exhibited increased functional connectivity of the insula with the right occipital lingual gyrus (p = 0.014, MNI: 18 −102 −3), the nucleus accumbens (p = 0.004, MNI: 33 3 -15), the left marginal lobe sulcal gyrus (p < 0.001, MNI: −27 0 −30), and the nucleus accumbens (p = 0.027, MNI: −12 9 −9) (Table 2, Fig. 4).

Table 2. Group comparison of functional connections based on insula as seed points.

ROI	Regions	T	MNI coordinate			Condition	P-FWE_corr
			x	y	z		
Insula	Right occipital lingual gyrus	4.64	18	−102	−3	NA > HC	0.000
Insula	Right nucleus accumbens	5.13	33	3	−15	NA > HC	0.014
Insula	Left marginal lobe sulcal gyrus	4.22	−27	0	−30	NA > HC	0.027
Insula	Left nucleus accumbens	5.07	−12	9	−9	NA > HC	0.004

MNI, Montreal Neurological Institute.

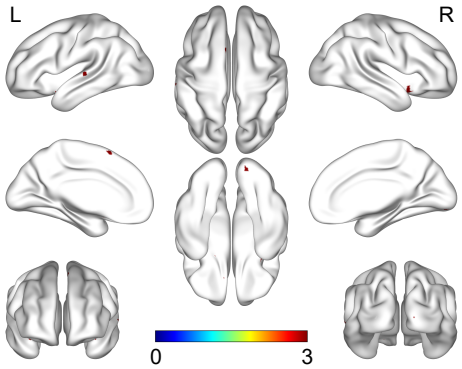

Fig. 4 Group differences in seed-based resting-state FC. The results were corrected for multiple comparisons (voxelwise p < 0.05, family-wise error [FWE] corrected).

Brain-behavior analysis

The radiomic features of IQR was correlated with the smoking index (r = 0.404, p = 0.013), years of smoking (r = 0.362, p = 0.015), and subjective craving (r = 0.320, p = 0.036), and Mean was correlated with age at first smoking/first cigarette (r = 0.302, p = 0.036). Enhanced functional connectivity of the insula with the sulcal gyrus of the left marginal lobe was negatively correlated with subjective cravings (r = −0.355, p = 0.023), and the FTND score (r = −0.356, p = 0.015). In addition, SRLGLE was correlated with enhanced insula and right occipital lingual gyrus functional connectivity (r = 0.288, p = 0.044) (Fig. 5).

Discussion

In this study, we investigated microstructural and functional magnetic resonance imaging measurements characterizing the insula in individuals addicted to nicotine and their relationships with different smoking characteristics. The AUC, SEN, SPE, and ACC values of the classification models that were built for the five identified radiomic features with different IQR, SZNU, Mean, SRLGLE, and SALGLE values were 0.9455, 0.9062, 0.9143, and 0.9104, respectively. Moreover, the AUC, SEN, SPE, and ACC values of the validation set were 0.8756, 0.7333, 0.7333, 0.7333, and 0.7333, respectively. Stable classification performance indicated that the defined radiomic features of the insula were able to differentiate smokers from nonsmokers. In addition, seed-based functional connectivity analysis revealed enhanced functional connectivity of the insula with the right occipital lingual gyrus (p = 0.014, MNI: 18 −102 −3), the nucleus accumbens (p = 0.004, MNI: 33 3 −15), the left marginal lobe sulcal

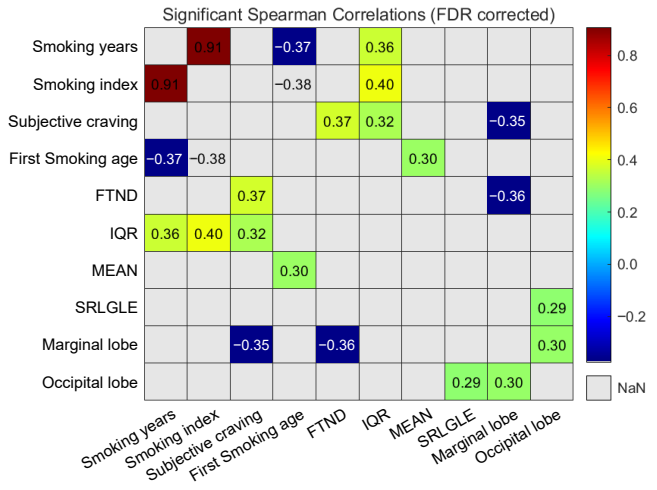

Fig. 5 Spearman correlation (FDR corrected) heat maps of imaging data and behavioral data.

gyrus ($p < 0.001$, MNI: −27 0 −30), and the nucleus accumbens ($p = 0.027$, MNI: −12 9 −9) in the smoking group compared with the nonsmoking group. Further correlation analysis revealed that IQR was correlated with the smoking index ($r = 0.404$, $p = 0.013$), years of smoking ($r = 0.362$, $p = 0.015$), and subjective craving ($r = 0.320$, $p = 0.036$), and that Mean was correlated with age at first smoking/first cigarette ($r = 0.302$, $p = 0.036$). Enhanced functional connectivity of the insula with the sulcal gyrus of the left marginal lobe was negatively correlated with subjective cravings ($r = -0.355$, $p = 0.023$) and the FTND score ($r = -0.356$, $p = 0.015$). SRLGLE was correlated with enhanced insula and right occipital lingual gyrus functional connectivity ($r = 0.288$, $p = 0.044$). Our measurements seem to support the idea that state-like smoking cravings and characteristic smoking clinical behaviors are correlated with microanatomical and functional measures and that microstructural changes exhibit some parallelism with functional changes on time scales.

In recent years, VBM and SBM methods have generally been used to investigate the brain structures of individuals with nicotine addictions in studies investigating the mechanisms of nicotine addiction; however, neither of these methods responds well to the characterization of brain regions. Although some studies have reported alterations in insula volume and the cortex in smokers, none of these findings have been consistent[28,32–34]. We attribute this to the low sensitivity of the measure, the singularity of the indicator, and the small sample size. Therefore, we used radiomics to capture the microscopic changes in the tissue structure of the insula in individuals with nicotine addictions and extracted radiomic features of the insula, from which we chose the five most differentiating indicators to build an SVM classification model to distinguish smokers from nonsmokers. Additionally, in the last two decades, there has been evidence[5] that damage to the insula makes it easier for nicotine-addicted individuals to succeed in the process of smoking cessation. Altered neural activity[35] in the insula has also been reported in short-term quitters. These studies demonstrated structural and functional changes in the insula in individuals with smoking addiction, and our study further explored the relationship between changes in insula microstructure and changes in functional connectivity.

Based on its location in the medial frontal, parietal, and temporal lobes, the insula is a brain region that is crucial for emotion regulation, self-awareness, and decision-making processes; moreover, alterations in the insula are strongly associated with addictive behaviors[3,4]. Our study confirms structural alterations in the insula in nicotine addiction and that these structural abnormalities can be better represented by high-dimensional radiomic features. Interestingly, we observed that microstructural changes of the insula were correlated with more clinical features of smoking. This finding is similar to a previous report[34] on the relationship between structural changes and clinical features; however, our finding differs from the results of a previous study[33] in which insula gray matter volume did not correlate with years of smoking. This difference may stem from the unique sensitivity of radiomic features, which are features extracted by image analysis techniques[15], usually reflecting the relationship between the distribution of gray levels of tissues in space and time, and providing a comprehensive anatomical representation of microstructural changes that are more sensitive to capture addiction-related neuroadaptive changes. Specifically, we found that the radiomic features of IQR were associated with smoking index, years of smoking, and subjective craving, and that Mean was associated with age at first smoking. Among the radiomic features, IQR reflects the variability or heterogeneity of the gray values within the tissue, with larger IQR values indicating greater variability and more complex structural features of the insula[36]. Tozer et al.[37] noted that the gray value coefficient of variation can reflect neurodegenerative processes such as glial cell proliferation or axonal remodeling, which provides a potential biological explanation for the association between years of smoking and elevated insula IQR. We hypothesized that higher smoking indices, longer years of smoking, and more intense cravings for smoking may lead to cellular proliferation in insula tissue. Mean, an index representing the average level of gray values in an image, reflects the overall characteristics of the tissue structure, and that early smoking behaviors may lead to alterations in the overall characteristics of the insula structure.

In terms of the relationship between clinical characteristics of smokers and insula functional connectivity, we found that enhanced insula functional connectivity with the left marginal lobe sulcus was negatively correlated with subjective craving and FTND scores. This finding is consistent with previous studies in which the insula has been repeatedly shown to be associated with smoking cravings[38] and to be involved in the nicotine addiction process, prompting researchers to train smokers to control the activity level in this region as a potential target for smoking cessation interventions. Chronic nicotine exposure may lead to dysregulation of information processing efficiency in the limbic system, and the insula maintains homeostatic balance by decreasing functional coupling to the limbic lobes, and Garrison et al.[39] suggested that altered functional connectivity of the insula in nicotine addicts may be a compensatory mechanism to reduce craving and impulsive behavior. In addition, we found that SRLGLE correlated with enhanced functional connectivity of the insula with the right occipital lingual gyrus. SRLGLE is used to characterize the intensity of short-running, low-gray-level regions in an image, thus reflecting the presence of low-brightness regions and their uniformity of distribution within the tissue. The positive correlation implies that when SRLGLE is elevated in the insula region, its microstructural changes support stronger functional connectivity, which correspondingly promotes the efficiency of addiction information processing. Thus, future studies could intensively explore the SRLGLE to help in revealing the mechanisms that are functioning in the addiction machinery, as well as its impact on cognitive function.

In this study, SVM classification model constructed from radiomic features successfully distinguished smoking and nonsmoking

populations, and the accuracy of the model was 0.9104, which was higher than previous classification models based on white matter structural or functional networks[40,41], demonstrating efficient discriminative efficacy. Previous studies have suggested that the insula can be a potential neuromodulatory target for addiction intervention, and our results further confirm the key role of the insula in smoking addiction behavior. In future studies, we can apply the sensitivity detected by radiomics to quantify the heterogeneous features of the insula subregion and further decode the neural mechanisms of nicotine addiction. In the future, a neuroimaging-assisted assessment system can be constructed to incorporate MRI scanning protocols (3D T1WI + rs-fMRI) in health checkups, and predictive modeling can be applied to help clinicians more accurately assess an individual's level of risk for smoking. However, such speculations need to be applied and generalized with caution, and further studies are needed to prove this.

Limitations

There are several limitations of this study: 1) There are potential baseline differences between smokers and non-smokers, such as age and education level, and these confounding variables may have an impact on the results of functional connectivity and radiomic features. Although indirectly controlling for these potential confounders may still limit the interpretation of the results. Good matching between groups should be done in future studies; 2) Modeling: Although 97 volunteers were recruited (50 smokers, 47 non-smokers), this may not have been sufficient to provide strong statistical power in the analysis and may have led to model overfitting. Radiomic features selected using Lasso regression may suffer from oversimplification, with an insufficient number of radiomic features incorporated into the model. Different feature selection methods may yield different results, so in the future, we should select radiomic features in larger samples and consider using other methods such as PCA or RFE to obtain more comprehensive feature selection results and validate the stability of the model; 3) This study lacked in-depth evaluation of pathological mechanisms, such as the pathological basis of key imaging markers, which can be further explored by combining genetic information and pathology in follow-up studies; 4) Our study was conducted with the whole insula as the region of interest, and a subregion of the insula was more heterogeneous in terms of radiomic features, which can be further clarified in the future; and 5) Cross-sectional studies cannot infer causality; longitudinal follow-up studies or controlled studies of nicotine addicts before and after quitting smoking are the way forward. These neuroimaging markers can be utilized to identify high-risk individuals, as well as to develop intervention strategies for them to enhance the success of smoking cessation.

Conclusions

In conclusion, through radiomics analysis, we explored radiomic features that can effectively identify nicotine-addicted populations. We also found that IQR correlates with subjective craving, and the insula has been repeatedly shown to correlate with smoking cravings[35]. Finally, SRLGLE correlated with enhanced insula functional connectivity with the right occipital lingual gyrus. Although our robustness to screening for radiomic features was average, the largely stable classification model helped us to explore the biological significance of radiomic features in nicotine addiction, and there is an imaging basis for consistent changes in the microstructure represented by radiomics and function represented by functional connectivity over time.

Ethical statements

The study was conducted in accordance with the Declaration of Helsinki, and the study protocol was approved by the Ethics Committee of Hunan Provincial People's Hospital (The First Affiliated Hospital of Hunan Normal University) (Approval No. 2021-72) in 2021. Informed consent for participation was obtained from all subjects involved in the study.

Author contributions

The authors acknowledge the following contributions to the paper: study conception and design: Xie A, Liao Y, Zheng H; data collection: Chen H, Zheng H, Zhu R, Huang F, Liu P; analysis and interpretation of the results: Zheng H, Gu Q; writing the manuscript: Zheng H, Xie A, Gu Q. All authors reviewed the findings and approved the final version of the manuscript.

Data availability

The data from the SHAPE cohort analyzed in this study are available from the corresponding author upon reasonable request.

Acknowledgments

This work was supported by the Outstanding Youth Fund Program of Hunan Provincial Department of Education (21B0083); and the Natural Science Foundation of Hunan Province (2025JJ80695).

Conflict of interest

The authors declare that they have no conflict of interest.

Dates

Received 24 December 2024; Revised 1 April 2025; Accepted 9 April 2025; Published online 24 April 2025

References

1. Yang JJ, Yu D, Wen W, Shu XO, Saito E, et al. 2019. Tobacco smoking and mortality in Asia: a pooled meta-analysis. *JAMA Network Open* 2:e191474
2. Le Foll B, Piper ME, Fowler CD, Tonstad S, Bierut L, et al. 2022. Tobacco and nicotine use. *Nature Reviews Disease Primers* 8:19
3. Regner MF, Tregellas J, Kluger B, Wylie K, Gowin JL, et al. 2019. The insula in nicotine use disorder: Functional neuroimaging and implications for neuromodulation. *Neuroscience & Biobehavioral Reviews* 103:414–24
4. Uddin LQ, Nomi JS, Hébert-Seropian B, Ghaziri J, Boucher O. 2017. Structure and function of the human insula. *Journal of Clinical Neurophysiology* 34:300–6
5. Abdolahi A, Williams GC, van Wijngaarden E. 2019. Implications of insular cortex laterality for treatment of nicotine addiction. *Drug and Alcohol Dependence* 201:178–81
6. Bellini BB, Scholz JR, Abe TO, Arnaut D, Tonstad S, et al. 2024. Does deep TMS really works for smoking cessation? A prospective, double blind, randomized, sham controlled study. *Progress in Neuro-Psychopharmacology and Biological Psychiatr* 132:110997
7. Ibrahim C, Rubin-Kahana DS, Pushparaj A, Musiol M, Blumberger DM, et al. 2019. The insula: a brain stimulation target for the treatment of addiction. *Frontiers in Pharmacology* 10:720
8. Chen Y, Chaudhary S, Wang W, Li CR. 2022. Gray matter volumes of the insula and anterior cingulate cortex and their dysfunctional roles in cigarette smoking. *Addiction Neuroscience* 1:100003

9. Bu L, Yu D, Su S, Ma Y, von Deneen KM, et al. 2016. Functional connectivity abnormalities of brain regions with structural deficits in young adult male smokers. *Frontiers in Human Neuroscience* 10:494
10. Hett K, Lyu I, Trujillo P, Lopez AM, Aumann M, et al. 2021. Anatomical texture patterns identify cerebellar distinctions between essential tremor and Parkinson's disease. *Human Brain Mapping* 42:2322–31
11. Betrouni N, Moreau C, Rolland AS, Carrière N, Chupin M, et al. 2021. Texture-based markers from structural imaging correlate with motor handicap in Parkinson's disease. *Scientific Reports* 11:2724
12. Lin F, Wu G, Zhu L, Lei H. 2019. Region-Specific Changes of Insular Cortical Thickness in Heavy Smokers. *Frontiers in Human Neuroscience* 13:265
13. Perez Diaz M, Pochon JB, Ghahremani DG, Dean AC, Faulkner P, et al. 2021. Sex Differences in the Association of Cigarette Craving With Insula Structure. *The International Journal of Neuropsychopharmacology* 24:624–33
14. Stamoulou E, Spanakis C, Manikis GC, Karanasiou G, Grigoriadis G, et al. 2022. Harmonization strategies in multicenter MRI-based radiomics. *Journal of Imaging* 8:303
15. Castellano G, Bonilha L, Li LM, Cendes F. 2004. Texture analysis of medical images. *Clinical Radiology* 59:1061–69
16. Haneberg AG, Pierre K, Winter-Reinhold E, Hochhegger B, Peters KR, et al. 2023. Introduction to radiomics and artificial intelligence: a primer for radiologists. *Seminars in Roentgenology* 58:152–57
17. Scapicchio C, Gabelloni M, Barucci A, Cioni D, Saba L, et al. 2021. A deep look into radiomics. *La Radiologia Medica* 126:1296–311
18. Gillies RJ, Kinahan PE, Hricak H. 2016. Radiomics: images are more than pictures, they are data. *Radiology* 278:563–77
19. Suoranta S, Holli-Helenius K, Koskenkorva P, Niskanen E, Könönen M, et al. 2013. 3D texture analysis reveals imperceptible MRI textural alterations in the thalamus and putamen in progressive myoclonic epilepsy type 1, EPM1. *PLoS One* 8:e69905
20. Zhang J, Tong L, Wang L, Li N. 2008. Texture analysis of multiple sclerosis: a comparative study. *Magnetic Resonance Imaging* 26:1160–66
21. Jiang J, Wang M, Alberts I, Sun X, Li T, et al. 2022. Using radiomics-based modelling to predict individual progression from mild cognitive impairment to Alzheimer's disease. *European Journal of Nuclear Medicine and Molecular Imaging* 49:2163–73
22. Péran P, Cherubini A, Assogna F, Piras F, Quattrocchi C, et al. 2010. Magnetic resonance imaging markers of Parkinson's disease nigrostriatal signature. *Brain* 133:3423–33
23. Li C, Li W, Liu C, Zheng H, Cai J, Wang S. 2022. Artificial intelligence in multiparametric magnetic resonance imaging: a review. *Medical Physicss* 49:e1024–e1054
24. Li Y, Yuan K, Guan Y, Cheng J, Bi Y, et al. 2017. The implication of salience network abnormalities in young male adult smokers. *Brain Imaging and Behavior* 11:943–53
25. Hutton C, Draganski B, Ashburner J, Weiskopf N. 2009. A comparison between voxel-based cortical thickness and voxel-based morphometry in normal aging. *Neuroimage* 48:371–80
26. Abbasian Ardakani A, Bureau NJ, Ciaccio EJ, Acharya UR. 2022. Interpretation of radiomics features - a pictorial review. *Computer Methods and Programs in Biomedicine* 215:106609
27. Heatherton TF, Kozlowski LT, Frecker RC, Fagerström KO. 1991. The Fagerström test for nicotine dependence: a revision of the Fagerström Tolerance Questionnaire. *British Journal of Addiction* 86:1119–27
28. Peng P, Wang Z, Jiang T, Chu S, Wang S, et al. 2017. Brain-volume changes in young and middle-aged smokers: a DARTEL-based voxel-based morphometry study. *The Clinical Respiratory Journal* 11:621–31
29. Kavzoglu T, Colkesen I. 2009. A kernel functions analysis for support vector machines for land cover classification. *International Journal of Applied Earth Observation and Geoinformation* 11:352–59
30. Kumar V, Gu Y, Basu S, Berglund A, Eschrich SA, et al. 2012. Radiomics: the process and the challenges. *Magnetic Resonance* 30:1234–48
31. Yan CG, Wang XD, Zuo XN, Zang YF. 2016. DPABI: data processing & analysis for (resting-state) brain imaging. *Neuroinformatics* 14:339–51
32. Wang C, Huang P, Shen Z, Qian W, Li K, et al. 2019. Gray matter volumes of insular subregions are not correlated with smoking cessation outcomes but negatively correlated with nicotine dependence severity in chronic smokers. *Neuroscience Letters* 696:7–12
33. Conti AA, Baldacchino AM. 2023. Early-onset smoking theory of compulsivity development: a neurocognitive model for the development of compulsive tobacco smoking. *Frontiers in Psychiatry* 14:1209277
34. Yang Z, Zhang Y, Cheng J, Zheng R. 2020. Meta-analysis of brain gray matter changes in chronic smokers. *European Journal of Radiology* 132:109300
35. Chen Y, Li CR. 2023. Overnight abstinence, Ventrostriatal-insular connectivity, and tridimensional personality traits in cigarette smokers. *Journal of Integrative Neuroscience* 22:66
36. Lambin P, Rios-Velazquez E, Leijenaar R, Carvalho S, van Stiphout RGPM, et al. 2012. Radiomics: extracting more information from medical images using advanced feature analysis. *European Journal of Cancer* 48:441–46
37. Tozer DJ, Zeestraten E, Lawrence AJ, Barrick TR, Markus HS. 2018. Texture Analysis of T1-Weighted and Fluid-Attenuated Inversion Recovery Images Detects Abnormalities That Correlate With Cognitive Decline in Small Vessel Disease. *Stroke* 49:1656–61
38. Bi Y, Yuan K, Guan Y, Cheng J, Zhang Y, et al. 2017. Altered resting state functional connectivity of anterior insula in young smokers. *Brain Imaging and Behavior* 11:155–65
39. Garrison KA, Sinha R, Lacadie CM, Scheinost D, Jastreboff AM, et al. 2016. Functional connectivity during exposure to favorite-food, stress, and neutral-relaxing imagery differs between smokers and nonsmokers. *Nicotine & Tobacco Research* 18:1820–29
40. Wetherill RR, Rao H, Hager N, Wang J, Franklin TR, et al. 2019. Classifying and characterizing nicotine use disorder with high accuracy using machine learning and resting-state fMRI. *Addiction Biology* 24:811–21
41. Fan C, Zha R, Liu Y, Wei Z, Wang Y, et al. 2023. Altered white matter functional network in nicotine addiction. *Psychiatry Research* 321:115073